Epithelial-to-Mesenchymal Transition in Early Transplant Tubulointerstitial Damage

Matthew J. Vitalone,* Philip J. O'Connell,† Elvira Jimenez-Vera,* Aysen Yuksel,‡ Moses Wavamunno,† Caroline L.-S. Fung,§ Jeremy R. Chapman,† and Brian J. Nankivell†

*Centre for Transplant and Renal Research and ‡Department of Histology, Westmead Millennium Institute, and Departments of †Renal Medicine and §Tissue Pathology, University of Sydney, Westmead Hospital, Sydney, Australia

ABSTRACT

It is unknown whether epithelial-to-mesenchymal transition (EMT) leads to tubulointerstitial fibrosis in renal transplants. In this study, interstitial fibrosis and markers of EMT were followed in protocol transplant biopsies in 24 patients. Tubulointerstitial damage (TID) increased from 34 to 54% between 1 and 3 mo after transplantation. Detection of EMT depended on the marker used; low levels of α-smooth muscle actin were found in 61% of biopsies, but the less specific marker S100 calcium binding protein-A4 (also known as Fsp1) suggested a higher incidence of EMT. The presence or development of TID did not correlate with EMT but instead significantly correlated with subclinical immune activity ($P < 0.05$). Among biopsies showing TID, microarray analysis revealed differential regulation of 127 genes at 1 mo and 67 genes at 3 mo compared with baseline; these genes were predominantly associated with fibrosis, tissue remodeling, and immune response. Of the 173 EMT-associated genes interrogated, however, only 8.1% showed an expression pattern consistent with EMT at 1 mo and 6.3% at 3 mo. The remainder were not differentially altered, or their changes in expression were opposite those expected to promote EMT. Quantitative reverse transcriptase–PCR revealed that the expression pattern of 12 EMT-associated genes was inconsistent over time, opposite that expected, or consistent with subclinical rejection or inflammation. In conclusion, EMT does not seem to play a significant role in the development of early allograft fibrosis.

J Am Soc Nephrol 19: 1571–1583, 2008. doi: 10.1681/ASN.2007050580

Chronic tubulointerstitial fibrosis is predominant in failing kidney allografts, increasing with time after transplantation and influencing graft function and survival.[1] Moderate transplant fibrosis present at 3 mo on protocol biopsy is associated with increased long-term graft loss.[2] Interstitial fibrosis is produced by activated myofibroblasts, and their origin is central to understanding the pathogenesis of progressive renal transplant damage. While some tubulointerstitial damage reflects a nonspecific end pathway of tubular cell injury with a limited repertoire of response, other specific mechanisms of fibrosis have been postulated, including epithelial-to-mesenchymal transition (EMT), whereby the tubular epithelial cells are precursors transitioning into interstitial myofibroblasts.

EMT is a highly regulated process whereby epithelial cells go through a series of programmed phenotypic changes, characterized by a loss of epithelial markers and function, migration into the extracellular space, and morphosis into a myofibroblast phenotype expressing α-smooth muscle actin (α-SMA). An important early step in this process is the loss of cell–cell adhesion (with downregulation of

Received May 17, 2007. Accepted February 13, 2008.

Published online ahead of print. Publication date available at www.jasn.org.

Correspondence: Dr. Brian J. Nankivell, Department of Renal Medicine, Westmead Hospital, Westmead, 2145, NSW, Sydney, Australia. Phone: +61-2-9845-6962; Fax: +61-2-9633-9351; E-mail: brian_nankivell@wsahs.nsw.gov.au

E-cadherin [ECAD]), followed by cellular elongation and breakdown of the basal lamina *via* matrix metalloproteinases 2 and 9 (MMP-2 and MMP-9).[3] This promotes cell migration through the extracellular matrix. These newly formed mesenchymal cells may take on a myofibroblast phenotype, secreting matrix proteins and initiating renal fibrosis.[4–7] Interest in the role of EMT in renal disease is increasing,[8,9] although its importance in kidney allograft fibrosis relative to the contributions of resident or infiltrating fibroblasts remains to be proved. This study aimed to investigate the role and significance of EMT in early transplant tubulointerstitial damage (TID) using the complementary technologies of immunohistochemistry and immunofluorescence, morphometric assessment of fibrosis, genome-wide microarray analysis, and quantitative real-time PCR, combined with prospective sequential protocol histology.

RESULTS

Interstitial Fibrosis and EMT Dual Staining

After classification of posttransplantation biopsies ($n = 61$) by the Banff criteria, 26 biopsies had a Banff score of ≥1 for both interstitial fibrosis and tubular atrophy (TID; formally referred to as chronic allograft nephropathy[10]), and 35 biopsies were normal (no TID). As expected, there was increased interstitial fibrosis quantified by morphometric analysis between normal biopsies and TID at 3 mo ($P = 0.039$; Figure 1A). More subclinical rejection was present at 1 and 3 mo in the TID cohort (36%; $P < 0.01$ *versus* no TID), with increased progression of interstitial fibrosis between 1 and 3 mo ($P < 0.05$).

EMT dual staining by α-SMA was seen in 41 of 67 biopsies (18 samples were exhausted), but this was not associated with a significant increase in the percentage of interstitial fibrosis ($r = 0.28$, $P = 0.11$; Figure 1B) on contemporaneous samples. Similarly, the incidence of EMT markers was no different at 1-mo protocol biopsies in patients with or without TID at 3 or 12 mo using sequential histology (Table 1). EMT dual staining by S100 calcium binding protein-A4 (S100A4) was seen in all posttransplantation biopsies to a variable degree (Figures 2, D through F, and 3B) but again was not associated with TID ($r = 0.21$, NS) or by sequential analysis (Tables 1 and 2).

Dual staining for ECAD and α-SMA was present in tubular and/or interstitial areas in 61% ($n = 41$ of 67) of biopsies (Figure 2, A through C); however, the intensity was relatively low (Tables 1 and 2, Figure 3A). Tubular EMT staining by α-SMA failed to correlate with intraluminal ($r = 0.19$, NS) or interstitial EMT ($r = 0.04$, NS), whereas interstitial α-SMA (suggestive of fibroblasts) per high-power field (HPF) correlated with Banff acute interstitial scores ($r = 0.33$, $P < 0.05$) and inflammation within areas of fibrosis ($r = 0.45$, $P = 0.011$) but not with dual staining of interstitial ($r = 0.04$, NS), tubular ($r = -0.08$, NS), or luminal cells ($r = 0.08$, NS). Dual tubular α-SMA staining per ECAD-positive tubule (ECAD tubule: Staining with ECAD only) correlated with fraction of interstitial fibrosis ($r = 0.56$, $P < 0.05$) at 1 mo but not at 3 mo ($r = -0.17$, NS) or with 1-yr Banff scores for interstitial fibrosis ($r = -0.32$, NS). Furthermore, there was no correlation in dual α-SMA staining between 1 and 3 mo for tubules ($r = -0.11$, NS), lumen ($r = 0.18$, NS), and interstitial areas ($r = -0.46$, NS); however, using tubular EMT dual staining by S100A4, there were no significant correlations between acute and chronic Banff scores (data not shown). Paradoxically, the degree of tubular dual S100A4 staining inversely correlated with serum creatinine at the biopsy time point ($r = -0.50$, $P < 0.001$), possibly explained by tubular injury reducing ECAD

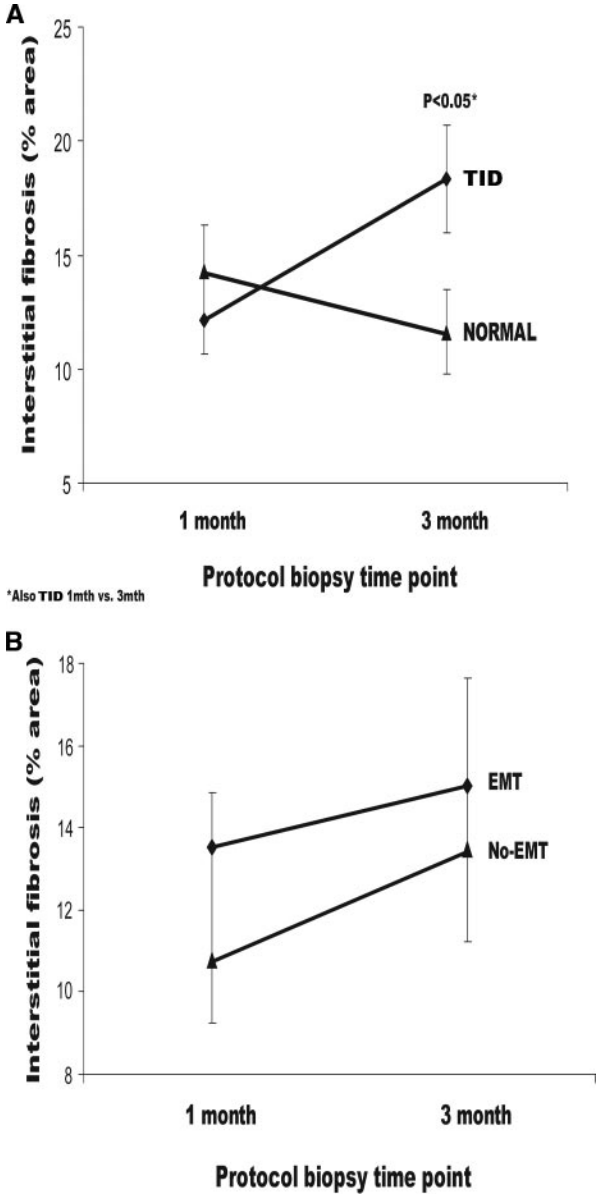

Figure 1. (A and B) Percentage area of interstitial fibrosis calculated on protocol biopsy and grouped according to TID (A) and EMT dual staining (α-SMA) (B). There was no association between EMT and interstitial fibrosis; TID was progressive and independent of EMT.

Table 1. Influence of EMT at 1 mo on subsequent 3-mo TID from sequential pathology series[a]

Group	TID	No TID	*P*
Three-month histologic parameters			
n (biopsies)	12	11	NS
serum creatinine (μmol/L; mean ± SD)	132.00 ± 44.00	104.00 ± 21.00	NS (<0.060)
interstitial fibrosis (ci score; mean ± SD)	1.00 ± 0.00	0.09 ± 0.30	<0.001
tubular atrophy (ct score; mean ± SD)	1.00 ± 0.00	0.30 ± 0.50	<0.001
Banff i score (mean ± SD)	0.59 ± 0.96	0.04 ± 0.20	<0.010
fibrotic inflammation (mean ± SD)	1.70 ± 1.00	0.15 ± 0.40	<0.001
One-month EMT markers (mean ± SD)			
dual staining for ECAD and α−SMA by immunoperoxidase			
dual stain/ECAD tubular cells	0.01 ± 0.01	0.01 ± 0.01	NS
dual tubular cells/HPF	0.50 ± 0.83	0.68 ± 1.32	NS
dual cells in tubular lumen/HPF	0.50 ± 0.97	0.22 ± 0.44	NS
dual cells in interstitium/HPF	0.30 ± 0.67	0.56 ± 1.01	NS
dual/αSMA interstitial cell	0.03 ± 0.04	0.02 ± 0.03	NS
dual staining for ECAD and S100A4 by immunofluorescence			
dual stain/ECAD tubular cells	0.16 ± 0.14	0.23 ± 0.18	NS
dual tubular cells/HPF	14.71 ± 12.47	21.33 ± 9.41	NS
dual cells in tubular lumen/HPF	0.14 ± 0.21	0.45 ± 0.96	NS
dual cells in interstitium/HPF	0.02 ± 0.06	0.00 ± 0.00	NS
dual/S100A4 interstitial cell	1.28 ± 1.67	3.21 ± 5.45	NS

[a]Three-month protocol biopsies were classified by the presence of histologically defined TID and compared with previous EMT parameters at 1 mo, defined by dual staining of ECAD and either α−SMA or S100A4. Counts expressed per HPF or by proportion of total ECAD-positive tubular cells. ci, chronic interstitial fibrosis; ct, chronic tubular atrophy; i, interstitial mononuclear cell inflammation.

expression generally. Interstitial S100A4 staining alone correlated strongly with Banff acute interstitial lymphocytic scores ($r = 0.49$, $P < 0.01$), tubulitis ($r = 0.48$, $P < 0.01$), inflammation within areas of fibrosis ($r = 0.52$, $P = 0.01$), Banff chronic interstitial fibrosis score ($r = 0.53$, $P < 0.001$) and tubular atrophy score (Banff chronic tubular atrophy, $r = 0.59$, $P < 0.001$). Hence, dual staining for EMT by either method was not associated with contemporaneous or subsequent interstitial fibrosis at 1 and 3 mo after transplantation, indicating that the myofibroblasts causing fibrosis were not originating from EMT-derived tubular cells.

cDNA Microarray Results and Programmed EMT

For determination of whether there was a programmed series of gene events controlling EMT in tubules, RNA from protocol biopsies ($n = 46$ biopsies, 35 paired arrays) was evaluated using cDNA microarrays against 8200 genes that included 173 genes identified from the published literature, associated with either EMT or the inverse mesenchymal-to-epithelial transition (MET) pathway (abridged representative list of the EMT/MET-associated genes, Table 3).

From biopsies demonstrating TID at 1 mo (compared with their respective implantation biopsy), 127 differentially expressed genes (B value >1, $P < 0.01$) were found, 14 (11%; Table 4) of which were associated with EMT. This represented only 8.1% of the EMT-associated genes present on the array. These consisted of fibrosis genes, such as collagens (extracellular fibrotic matrix), MMP-2 and its inhibitor TIMP2 (extracellular matrix remodeling), fibroblast activation and IGF (signaling molecules), and Cyclin I (cell cycle).

In addition, within these differently expressed EMT genes, several anomalies were identified. Tissue inhibitor of matrix metallopeptidase 2 (TIMP2) and collagen VIII α-2 (COL8A2) were upregulated instead of being downregulated, as would be expected from EMT activation. Large numbers of key initiating factors of EMT, such as TGF-β superfamily signaling molecules and receptors, transcription factors such as *mothers* against DDP homolog 2/3 or 4 (*Drosophila*), SMAD2/3 or 4 and Snail, various myofibroblast specific transcripts such as α-SMA and vimentin, along with mitogen-activated protein kinase family of genes, were not differentially expressed. Similarly, the inverse MET pathway genes were not differentially expressed (Tables 3 and 4). Analysis of 3-mo protocol biopsies showing TID where 67 differentially expressed genes (B > 1, $P < 0.015$) were found confirmed that only 15% of genes (Table 4) were associated with EMT, representing 6.3% of the EMT genes on the array. Again, TIMP2 expression was contrary to expectation, whereas TGF-β receptor 3 and CTGF (Table 4) were repressed, they have been reported as part of the initiating membrane complex in EMT and should have been induced.[3] Furthermore, when the differentially expressed genes in the TID cohort were subject to hierarchical clustering, there was no obvious grouping of EMT samples (data not shown). These findings indicated that most of the differentially expressed genes in early protocol kidney transplant biopsies were unrelated to EMT and that very few of the gene changes associated with EMT were present.

Quantitative Reverse Transcriptase-PCR Validated Microarray Gene Expression Results and Did not Support EMT-Associated Gene Expression in TID

QRT-PCR validated the results expressed by the microarray data for the three genes investigated: COL1A2, IGF2, and

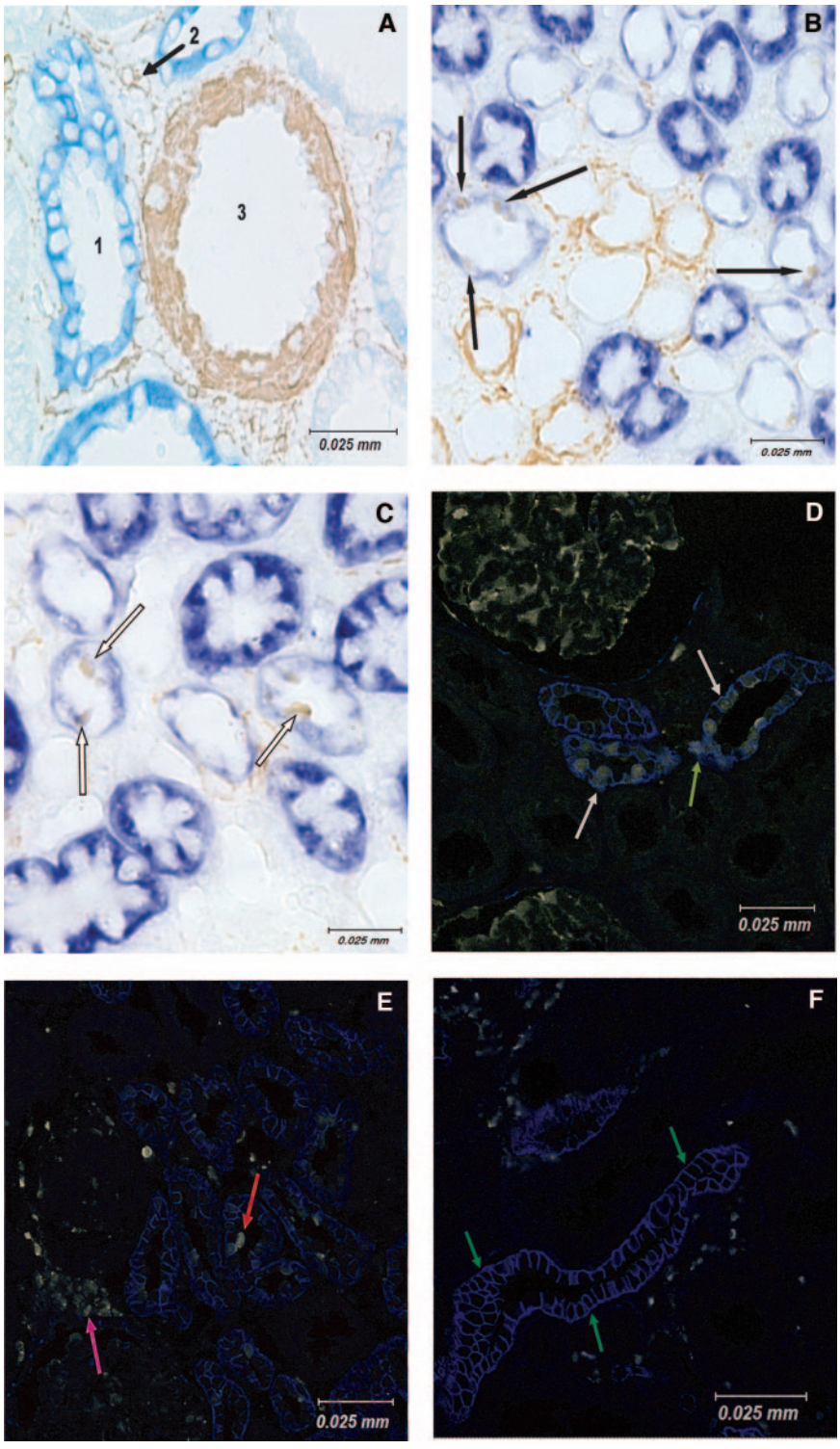

Figure 2. EMT evaluated by dual staining with ECAD and α-SMA (immunohistochemistry) or S100A4 (confocal immunofluorescence). (A) Normal biopsy showing singular staining of tubular epithelial cell (1) with ECAD (blue) and myofibroblast (2) and of small muscular vessel (3) with α-SMA (brown). (B and C) Single cells exhibiting dual-staining EMT using α-SMA were observed in the tubules (B, black arrows) and tubular lumen (C, white arrows) and projecting pseudopodia into the interstitium. (D and E) Dual staining using ECAD (blue) and S100A4 (yellow) showed EMT in single cells were observed in the tubules (D, white arrows), projecting pseudopodia into the interstitium (D, green arrow) and the tubular lumen (E, red arrow). (E) Singular staining with S100A4, indicating fibroblasts, was observed in the interstitium (pink arrow). (F) A normal tubule showing ECAD (blue) staining to the basal lateral border of the tubular epithelial cells (green arrows).

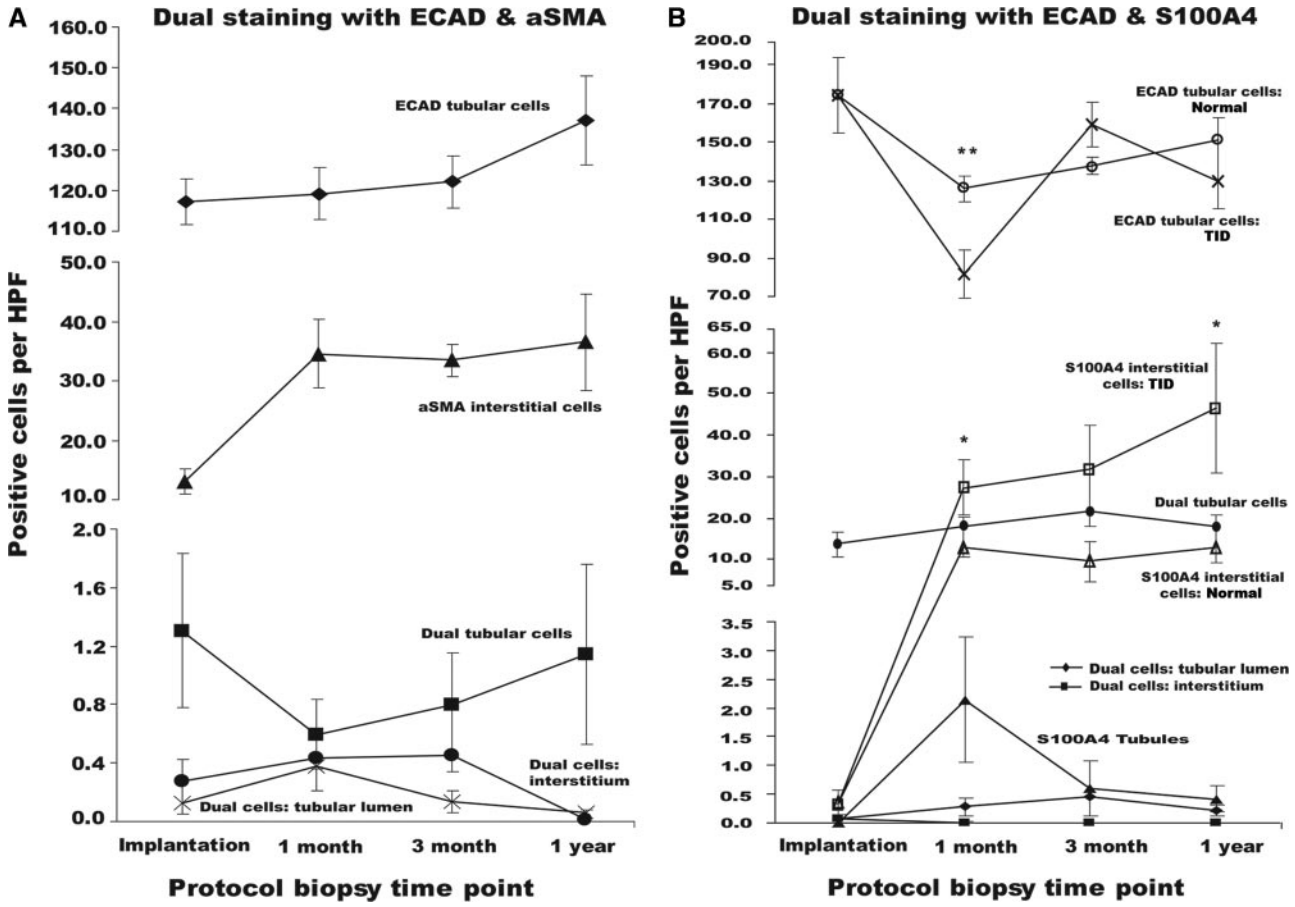

Figure 3. The degree of EMT was assessed by calculating the number of positive dual-stained cells per HPF using ECAD with α-SMA (immunohistochemistry) or S100A4 (confocal immunofluorescence). (A) Using α-SMA, only relatively low levels of dual-staining EMT were observed (>1.6 cells/HPF) during the first 12 mo after transplantation. Cells with singular staining of ECAD did not change during time, in the presence of an increase in α-SMA–positive myofibroblasts. (B) Using S100A4, varying levels of dual-staining EMT were observed but remained constant during the first 12 mo after transplantation, despite an increase of S100A4 interstitial fibroblasts with TID at 1 and 12 mo ($P = 0.05$ for both); 3 mo was just below significance ($P = 0.09$). Cells with singular staining of ECAD were decreased with TID at 1 mo ($P = 0.01$) but recovered to baseline by 3 mo.

RGPS3 (assessed to be highly significant by the arrays). These genes mirrored the fold change expression as calculated by the arrays; however, the microarrays consistently overestimated the fold change gene expression by a 1 to 2 orders of magnitude compared with QRT-PCR ($n = 55$).

Stratifying the data on the basis of the presence or absence of TID on biopsy demonstrated a small proportion of significantly expressed genes. Using Mann-Whitney *U*/Wilcoxon tests for significance, S100A4 ($P = 0.015$; Figure 4A) and β-catenin (BCAT; $P = 0.019$; Figure 4B) were upregulated at the 1-mo TID time point compared with normal biopsies. This is contrary to the expected repression of BCAT during EMT. This significance disappeared at 3 mo (S100A4 [$P = 0.25$] and BCAT [$P = 0.96$]). RGPS3 was also upregulated in the TID cohort ($P = 0.05$). All other EMT- or MET-related gene expression was not significantly different at either 1 or 3 mo after transplantation between TID and normal biopsies (Figure 4, C and D). We also observed an overall increase in COL1A2 and MMP-2 at 3 mo compared with implantation (Figure 4D), which fits with fibrosis and matrix remodeling; however, when the samples were stratified for the presence of TID, there was no significant difference compared with normal. Furthermore, the raw QRT-PCR expression data were analyzed by hierarchical clustering; similarly to the microarray results, there was no obvious grouping of EMT samples (data not shown).

Analyzing the data on the basis of categorical grouping, SNAI2 ($P = 0.031$), a major EMT transcription factor, had a significant tendency to two-fold or greater change in the TID group. There was no significant tendency to altered gene expression for any of the other genes in TID when compared with normal.

Using Pearson correlations. we observed that S100A4, a general fibroblast marker, correlated with the incidence of TID ($r = 0.38$, $P = 0.031$), particularly with Banff chronic interstitial fibrosis score ($r = 0.41$, $P = 0.019$). S100A4 also correlated with mesangial matrix ($r = 0.38$, $P = 0.029$) and dual staining with ECAD/α-SMA ($r = 0.41$, $P = 0.044$). This further supports the identification of transitioning myofibroblasts by dual

Table 2. Clinical outcome of groups classified according to the presence of EMT on 1-mo protocol classified by dual staining of ECAD by either α-SMA (by immunoperoxidase) or S100A4 (by immunofluorescence)

Group	EMT	No EMT	*P*
Dual Staining for ECAD and α-SMA by Immunoperoxidase			
no. of patients	11	8	NS
dual stain tubular cells/ECAD (mean ± SD)	0.62 ± 1.10	0.89 ± 1.80	NS
dual tubular cells/HPF (mean ± SD)	1.43 ± 2.00	0.00 ± 0.00	<0.001
dual cells in tubular lumen/HPF (mean ± SD)	0.31 ± 0.63	0.00 ± 0.00	<0.050
dual cells in interstitium/HPF (mean ± SD)	0.60 ± 0.80	0.00 ± 0.00	<0.001
3-mo ci score (mean ± SD)	0.36 ± 0.51	0.57 ± 0.53	NS
3-mo interstitial fibrosis (%; mean ± SD)	14.60 ± 7.20	14.50 ± 8.70	NS
1-yr ci score (mean ± SD)	0.33 ± 0.50	1.00 ± 1.70	NS
1-yr interstitial fibrosis (%; mean ± SD)	11.40 ± 5.60	19.50 ± 9.30	NS
1-yr serum creatinine (μ mol/L; mean ± SD)	121.00 ± 41.00	107.00 ± 42.00	NS
Dual staining for ECAD and S100A4 by immunofluorescence	Severe EMT	Minor/Absent EMT	*P*
no. of patients	10	9	NS
dual stain tubular cells/ECAD (mean ± SD)	0.27 ± 0.17	0.11 ± 0.08	<0.050
dual tubular cells/HPF (mean ± SD)	26.10 ± 8.60	8.60 ± 5.00	<0.001
dual cells in tubular lumen/HPF (mean ± SD)	0.43 ± 0.90	0.13 ± 0.13	NS
dual cells in interstitium/HPF (mean ± SD)	0.02 ± 0.06	0.00 ± 0.00	NS
3-mo ci score (mean ± SD)	0.50 ± 0.53	0.67 ± 0.50	NS
3-mo interstitial fibrosis (%; mean ± SD)	13.80 ± 7.60	14.80 ± 7.40	NS
1-yr ci score (mean ± SD)	0.16 ± 0.40	1.33 ± 1.50	NS (<0.100)
1-yr interstitial fibrosis (%; mean ± SD)	13.10 ± 5.50	14.00 ± 10.40	NS
1-yr serum creatinine (μ mol/L; mean ± SD)	91.00 ± 20.00	116.00 ± 45.00	NS

staining with ECAD/α-SMA; however, SMAD2, an intracellular marker (transcription factor) for EMT, negatively correlated with interstitial α-SMA staining ($r = -0.49$, $P = 0.015$), suggesting that infiltrating myofibroblasts were not originating from EMT-derived tubular cells. BCAT, an intracellular marker for MET, negatively correlated with dual staining of ECAD/α-SMA ($r = -0.61$, $P = 0.002$), supporting the evidence that dual staining was demonstrating isolated EMT events present in the biopsies. Hence, the QRT-PCR results showed no consistent pattern that would support a major role of EMT in the early development of fibrosis in TID.

DISCUSSION

This study demonstrates that EMT was present in renal transplantation, with prevalence rates dependent on the method used for assessment. With the use of α-SMA, a mesenchymal marker, dual staining was present at low levels with a small percentage of tubular epithelial cell showing EMT changes, whereas with the use of a general fibroblast marker S100A4 in dual staining, all of the protocol biopsies showed EMT of varying degrees; however, neither method of EMT detection at 1 mo predicted subsequent tubulointerstitial fibrosis at 3 or 12 mo, raising doubts as to its clinical relevance. Chronic interstitial fibrosis has been shown to be the end result of multiple immune and nonimmune insults, mediated by interstitial fibroblasts, and predicts long-term functional outcome[1,2]; however, the source of this fibrosis remains controversial: Whether it originates from host-derived infiltrating mesenchymal cells, activation of resident fibroblasts, or by transition of donor-derived tubular cells *via* EMT. EMT was proposed as an important mechanism in induction of TID[8,11]; however, EMT as a pathologic entity and its importance as a cause of renal fibrosis remain unproved. Our prospective study, using a variety of complementary techniques including dual-stained immunohistochemistry and immunofluorescence, morphometric analysis, QRT-PCR, and genome-wide microarray analysis of the transcriptome on protocol biopsies, failed to demonstrate a major role for EMT in the pathogenesis of early renal allograft tubulointerstitial fibrosis, although a more significant role at later time points in this process could not be excluded.

The key histopathologic feature of EMT is the dual staining of cells with ECAD (the main adherin junction protein joining adjacent tubular epithelial cells) and a myofibroblast marker (*e.g.*, α-SMA).[4,12] This is thought to represent the transition phase toward the myofibroblast linage. We observed dual EMT staining in tubules, sloughed cells within the tubular lumen and in the interstitium, although levels were low with the α-SMA/ECAD histochemistry (averaging 0.6 to 2.0 dual positive cells per HPF), which is the terminal EMT marker for myofibroblasts. A substantial increase of positive cells was identified using S100A4 dual staining, a general fibroblast marker that is not specific for myofibroblasts. EMT using α-SMA showed a very weak association with interstitial fibrosis at 1 mo only, despite progressive tubulointerstitial damage occurring between 1 and 3 mo after transplantation. Furthermore, there was no causal relationship between EMT (using either marker of S100A4 or α-SMA), with an increase in TID on two subsequent protocol biopsies at 3 and 12 mo. Myofi-

Table 3. An abridged representative gene expression list of the 173 EMT- or MET-associated genes present on the cDNA microarrays, assessed by LIMMA for significance[a]

Unigene ID	Name	Symbol	Gene Ontology and Function	Fold Change	*P*	B	EMT
Hs0.500483	Actin, α 2, smooth muscle	ACTA2	Actin filament/constituent of CSk	0.0936	0.7570	−6.222	+
Hs0.642645	Advanced glycosylation end product–specific receptor	AGER	Cell surface receptor linked signal transduction	−0.1830	0.6420	−5.823	+
Hs0.473163	Bone morphogenetic protein 7	BMP7	CDef	−0.0710	0.7640	−6.252	−
Hs0.524477	Bone morphogenetic protein receptor, IA	BMPR1A	TGF-βRSP	−0.3430	0.4880	−5.588	−
Hs0.471119	Bone morphogenetic protein receptor, type II (serine/threonine kinase)	BMPR2	TGF-βRSP	−0.2110	0.6700	−5.994	−
Hs0.461086	Cadherin type 1, E-cadherin (epithelial)	CDH1	Cad	−0.0740	0.8080	−6.227	−
Hs0.76206	Cadherin 5, type 2, VE-cadherin (vascular epithelium)	CDH5	Cad	0.0340	0.9140	−6.408	−
Hs0.476018	Catenin (cadherin-associated), β 1	CTNNB1	Wnt receptor signaling pathway/Cad	−0.2400	0.5320	−5.650	−
Hs0.489142	Collagen, type I, α 2	COL1A2	Cad/ECM structural constituent	3.9320	5.6e-6	12.337	+
Hs0.443625	Collagen, type III, α 1	COL3A1	Cad/ECM structural constituent	4.0190	3.4e-5	9.8603	+
Hs0.410037	Connective tissue growth factor	CTGF	Cad/regulation of cell growth	−0.4400	0.2690	−4.645	+
Hs0.642729	Cyclin I	CCNI	Regulation of cell cycle	0.8511	0.0049	2.687	+
Hs0.419815	Epidermal growth factor (β-urogastrone)	EGF	Activation of MAPK/+CPro	−0.8240	0.2215	−4.308	+
Hs0.488293	Epidermal growth factor receptor	EGFR	CPro/EGFR activity	−0.3120	0.1188	−3.253	+
Hs0.516493	Fibroblast activation protein α	FAP	CPro	1.7943	0.0065	2.203	+
Hs0.264887	Fibroblast growth factor 1 (acidic)	FGF1	Angiogenesis/CDef/CPro	−0.1990	0.5053	−5.554	+
Hs0.264887	Fibroblast growth factor receptor 1	FGFR1	Cell growth/FGFR activity	0.4828	0.2417	−4.460	+
Hs0.9914	Follistatin	FST	Activin inhibitor activity/Dev	0.4735	0.2105	−4.214	+
Hs0.592020	Insulin-like growth factor 1 receptor	IGF1R	EGFR activity/+CPro	−0.0640	0.6930	−6.101	+
Hs0.523414	Insulin-like growth factor 2	IGF2	CPro/Dev	1.9740	0.0001	8.090	+
Hs0.505654	Integrin, α 5 (fibronectin receptor)	ITGA5	Cad/integral to membrane	0.3820	0.1336	−3.500	+
Hs0.80828	Keratin 1 (epidermolytic hyperkeratosis)	KRT1	Angiogenesis/CSk	0.0789	0.6828	−6.130	−
Hs0.513617	Matrix metallopeptidase 2 (gelatinase A)	MMP2	Collagen catabolism	1.9590	0.0015	4.7438	+
Hs0.297413	Matrix metallopeptidase 9 (gelatinase B)	MMP9	Collagen catabolism	0.0451	0.8402	−6.020	+
Hs0.164384	Plakophilin 2	PKP2	Cad/CSk	−0.0490	0.9167	−6.442	+
Hs0.519005	SMAD, mothers against DPP homolog 1	SMAD1	BMPSP/TGF-βRSP	−0.0420	0.8829	−6.376	−
Hs0.12253	SMAD, mothers against DPP homolog 2	SMAD2	RT/TGFβRSP	−0.2430	0.2429	−4.472	+
Hs0.36915	SMAD, mothers against DPP homolog 3	SMAD3	RT/TGF-βRSP	0.0641	0.9535	−6.432	+
Hs0.75862	SMAD, mothers against DPP homolog 4	SMAD4	RT/TGF-βRSP/BMPSP	−0.1270	0.6237	−5.957	Both
Hs0.167700	SMAD, mothers against DPP homolog 5	SMAD5	BMPSP/TGF-βRSP	−0.2340	0.6498	−6.023	−
Hs0.48029	Snail homolog 1	SNAI1	Dev	0.0365	0.8855	−6.378	+
Hs0.104839	TIMP metallopeptidase inhibitor 2	TIMP2	Metalloendopeptidase inhibitor activity	0.8572	0.0029	3.4631	−
Hs0.155218	Transforming growth factor, β 1	TGFB1	CPro/CCS	0.0071	0.9836	−5.994	+
Hs0.2025	Transforming growth factor, β 3	TGFB3	CPro/CCS/organogenesis	0.7382	0.1331	−3.492	+
Hs0.82028	Transforming growth factor, β receptor II	TGFBR2	+CPro/ST	−0.1500	0.3761	−5.169	+
Hs0.482390	Transforming growth factor, β receptor III (betaglycan)	TGFBR3	+CPro/ST/Dev	−0.3840	0.1601	−3.787	+
Hs0.644998	Twist homolog 1	TWIST1	CDef/morphogenesis	−2.7040	0.0356	−1.061	+
Hs0.533317	Vimentin	VIM	CSk	−0.0180	0.9795	−5.808	+

[a]The vast majority of the EMT/MET-associated genes did not show significant differential gene expression at 1 or 3 mo after transplantation in TID samples. $B > 1$ and adjusted $P < 0.05$ are considered statically significantly differentially expressed. Fold change is estimated by the statistical package, which is expressed as a $\log_2$ fold change in gene expression. The gene expression transcriptome profile is unsupportive of EMT presence in early TID. BMPSP, bone morphogenic protein signaling pathway; Cad, cell adhesion; CCS, cell–cell signaling; CDef, cell differentiation; CSk, cytoskeleton; Dev, development; ECM, extracellular matrix; MAPK, mitogen-activated protein kinase; RT, Regulation of transcription; ST, signal transduction; TGF-βRSP, TGF-β receptor signaling pathway; +CPro, positive regulation of cell proliferation.

broblasts (identified by α-SMA or S100A4 staining) correlated with inflammatory cells in the cortex and within areas of fibrotic damage but not with EMT markers, suggesting an origin other than donor-tubular cells.

EMT is known to be controlled by a highly programmed cascade of intracellular events, initiated by many pleiotropic signals. The binding of lymphoid enhancer factor-1 with BCAT to form a complex suppresses ECAD, actin, and vimentin and inhibits cell adhesion leading to EMT.[13,14] Alternatively, binding of TGF-β with its cell surface receptor, followed by activation and nuclear translocation of SMAD (2/3/4) proteins, also results in EMT.[13,15,16] Occasionally, reactive oxygen species activate EMT with cytoskeletal disruption and loss of cell-to-cell interactions.[16] We searched for evidence of the intricate and highly regulated signaling molecules that lead from transition of tubular epithelial cells into myofibroblasts and control EMT. Analysis of expression profiles using an 8200-gene microarray was undertaken to determine whether tubular cells (containing most of the nucleic acids in a kidney biopsy) expressed any of the 173 recognized EMT/MET-associated genes. Of the 193 (cumulatively) differentially expressed genes in biopsy samples with tubulointerstitial fibrosis, only a small proportion were EMT associated, and these were fibrotic and signaling genes, which are readily explained by the presence of infiltrating fibroblasts, immune mechanisms, or tissue remodeling.

Not only was there a lack of differential expression of most of the expected initiating and transcription factors essential for the programmed progression of EMT (including TGF-β su-

Table 4. EMT- or MET-associated genes that were significantly differentially expressed ($B > 1$, $P < 0.014$) in protocol biopsies exhibiting TID pathology at 1 or 3 mo after transplantation, assessed by LIMMA[a]

Unigene ID	Gene Name	Fold Change	Adjusted *P*	B	Predicted Change with EMT
Differentially expressed genes at 1 mo with TID					
Hs0.489142	Collagen, type I, α2	3.93	5.59e-6	12.33	Up
Hs0.443625	Collagen, type III, α1	4.02	3.41e-5	9.86	Up
Hs0.523414	Insulin like growth factor 2 (somatomedin A)	1.97	1.4e-4	8.09	Up
Hs0.169047	chondroitin sulfate proteoglycan 2 (versican)	1.64	1.4e-4	7.99	Up
Hs0.474053	Collagen, type VI, α1	1.80	1.8e-4	7.48	Up
Hs0.420269	Collagen, type VI, α2	1.35	7.8e-4	5.77	Up
Hs0.513617	Matrix metallopeptidase 2 (gelatinase A)	1.96	0.0015	4.74	Up
Hs0.104839[b]	TIMP metallopeptidase inhibitor 2	0.86	0.0029	3.46	Down
Hs0.642729	Cyclin I	0.85	0.0049	2.68	Up
Hs0.516493	Fibroblast activation protein α	1.79	0.0065	2.20	Up
Hs0.134830[b]	Collagen, type VIII, α1	0.67	0.0073	1.93	Down
Hs0.233240	Collagen, type VI, α3	2.17	0.0073	1.89	Up
Hs0.210283	Collagen, type V, α1	1.77	0.0077	1.61	Up
Hs0.647231	EGF-containing fibulin-like extracellular matrix protein 2	0.42	0.0100	1.11	Up
Differentially expressed genes at 3 mo with TID					
Hs0.410037[b]	Connective tissue growth factor	−1.24	5.37e-6	12.47	Up
Hs0.302963	Spondin 2, extracellular matrix protein	1.43	2.11e-4	7.54	Up
Hs0.489142	Collagen, type I, α2	2.97	0.0025	4.86	Up
Hs0.644998	Twist homolog 1(*Drosophila*)	0.75	0.0051	2.93	Up
Hs0.443625	Collagen, type III, α1	2.88	0.0073	2.53	Up
Hs0.420269	Collagen, type VI, α2	0.91	0.0091	2.21	Up
Hs0.104839[b]	TIMP metallopeptidase inhibitor 2	0.56	0.0100	2.07	Down
Hs0.233240	Collagen, type VI, α3	1.67	0.0140	1.32	Up
Hs0.210283	Collagen, type V, α1	1.08	0.0140	1.14	Up
Hs0.482390[b]	Transforming growth factor, β receptor III	−0.58	0.0140	1.10	Up

[a]The majority of the main EMT-associated genes were not significantly differentially expressed. These few significantly differentially expressed EMT/MET-associated genes represented only 11 and 15%, respectively, of overall gene expression and 8.1 and 6.3%, respectively, of the 173 EMT-associated genes in 1 and 3 mo TID samples. $B > 1$ and adjusted $P < 0.05$ are significantly differentially expressed. Fold change is $\log_2$ fold change in gene expression.
[b]Expression opposite to expected changes during EMT and therefore are unsupportive of programmed EMT in TID.

perfamily, the SMAD, SNAIL [SNAI2], lymphoid enhancer factor-1 intercellular proteins. or mitogen-activated protein kinases), but similarly the inverse MET pathway was not represented. These genes are characteristically repressed with EMT, including bone morphogenic protein 7; bone morphogenic protein receptors 1 and 2; SMAD 1, 5, and 8 transcription factors; BCAT; cadherin-associated molecules; and cell adhesion molecules such as integrins. Indeed, in some instances, gene expression was opposite to what one would expect of EMT. For instance, TIMP2 and COL8A2 were activated in association with tubulointerstitial damage, whereas CTGF and TGF-β receptor 3 were repressed. In addition, microarrays failed to demonstrate α-SMA mRNA expression, although it was present by immunohistochemistry in localized positive α-SMA–expressing cells. This may be explained by the low frequency of such events even where detected histologically (see Tables 1 and 2). Hence, α-SMA mRNA may be swamped by other varying levels of gene expression signals from the heterogeneous population of cells in the graft biopsy. Other studies have also observed a discrepancy between mRNA and protein expression.[17,18] Posttranslational regulation, such as microRNA, may also explain differences in results between technologies.[19–21] The recognized reduced sensitivity of microarrays, especially cDNA arrays, leading to false-positive or -negative results, can be overcome by validation using QRT-PCR.[22,23] This validation step was done in this study and confirmed the array data. Hence, both QRT-PCR and genome-wide transcriptome analysis did not identify a gene expression pattern consistent with EMT activity, despite progressive posttransplantation interstitial fibrosis.

As part of the validation process, QRT-PCR of 12 selected important EMT/MET-associated genes was performed on implantation and 1- and 3-mo allograft samples. The gene expression pattern of these 12 genes was inconsistent across time points, was opposite to what one would expect in EMT, or represented nonspecific upregulated gene expression as a result of subclinical rejection or inflammation. For instance, S100A4 gene expression is consistent with the presence of fibroblasts but not specific for EMT. SNAI2, an EMT-associated transcription factor, did show a

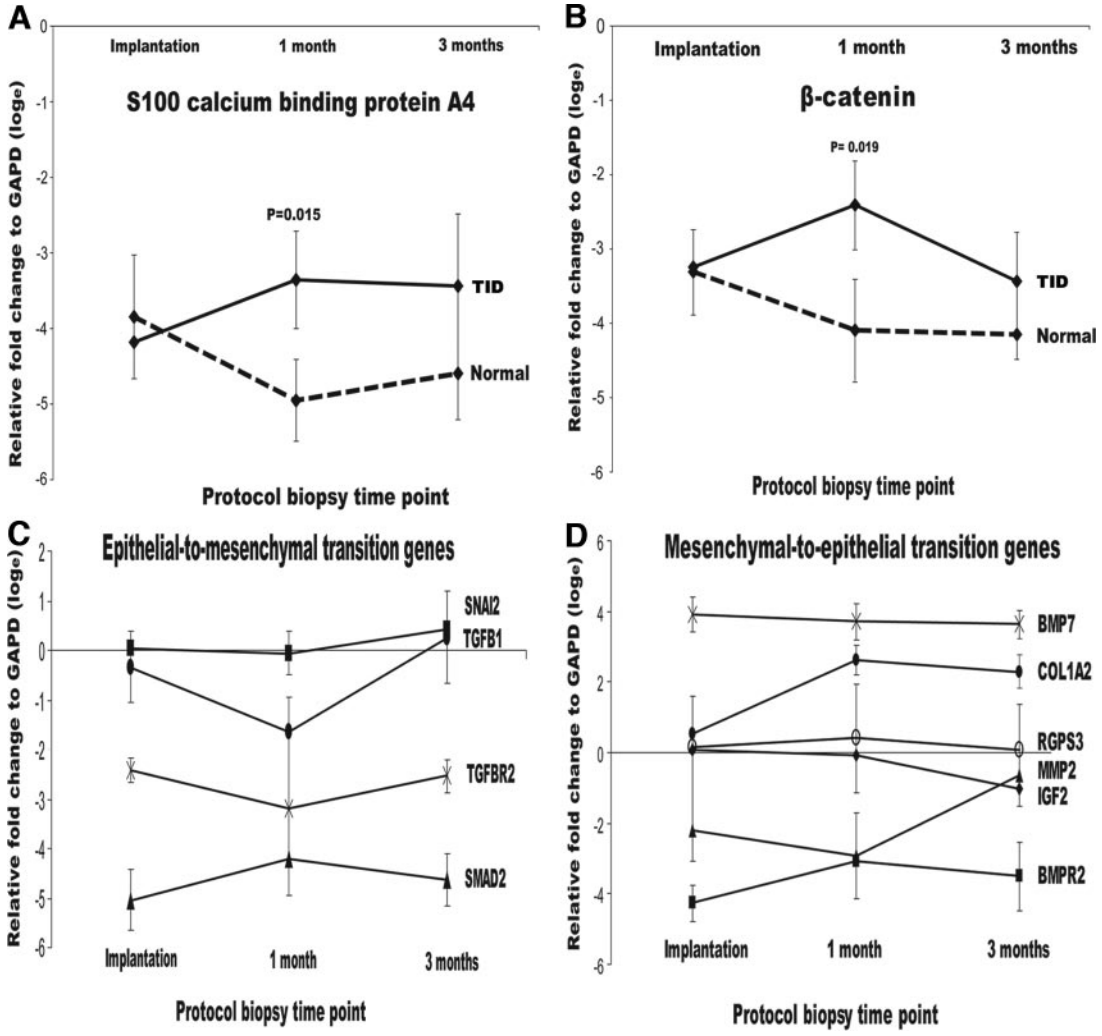

Figure 4. QRT-PCR assessment of 12 EMT- and MET-associated genes corrected against the housekeeper glyceraldehyde-3-phosphate dehydrogenase (GAPD). Of the 12 EMT/MET-associated genes, only four exhibited significant upregulation in the TID group. (A) S100A4 is a general fibroblast marker that is due to infiltrating myofibroblasts. B) BCAT (should be downregulated in EMT and therefore is in the wrong direction. (C and D) Furthermore, the remaining eight important genes show no significant gene expression, supporting EMT in TID samples. QRT-PCR transcriptome profile is unsupportive of EMT presence in early TID. Fold change is expressed as $\log_e$ to GAPD.

tendency to upregulation in TID but is insufficient evidence alone for EMT. Furthermore, SNAI2 expression is best explained by the association of EMT with rejection and T cell infiltration in previous studies[24,25] and the positive association with subclinical rejection and TID in this study, which was relatively low in occurrence in our study. By contrast, the significant upregulation of BCAT (MET marker/transcription factor) in TID and the negative correlation of SMAD2 expression with dual staining (EMT) argue against a role for EMT. Finally, hierarchical clustering of both microarray and QRT-PCR expression data sets failed to show any grouping on the basis of EMT dual staining, further supporting the view that EMT was not the predominant pathologic process causing early tubulointerstitial fibrosis.

Despite the importance of progressive fibrosis in chronic renal allograft injury, there have been relatively few studies of its etiology in renal transplant biopsies. In a small study of gender-mismatched recipients, a substantial proportion (24 to 40%) of infiltrating myofibroblasts within the neointima, adventitia, and interstitium of graft biopsies were found to be of donor origin. This was interpreted as showing that a significant proportion of graft fibrosis was the result of circulating recipient myofibroblasts rather than the result of EMT by donor tubular cells.[26] It was proposed that myofibroblast transformation may have been aggravated by early cyclosporine (CsA) toxicity. This was later supported by two *in vitro* studies showing that high levels of CsA given to cultured proximal tubular cells induced EMT and produced a fibrotic expression profile using microarrays.[27,28] Another possibility is that tubular epithelial cells undergoing EMT fail to migrate across the tubular

basement membrane into the interstitial space but instead, after losing their ECAD anchors, are sloughed into the tubular lumen, as we and others have observed.

Previous cross-sectional studies that proposed EMT as an important mechanism for renal allograft fibrosis relied predominantly on histochemical evidence of dual staining with epithelial and mesenchymal markers in renal tubular epithelial cells from biopsies with TID. In many instances, these changes were in association with cellular infiltrates and tubulitis, suggesting that tubular epithelial damage was an important factor for these changes.[9,25,29] Vongwiwatana *et al.*[8] compared clinically indicated biopsies undertaken relatively late in the life of the graft with immunohistochemical evidence of EMT to normal biopsies. In biopsies in which tubules seemed to be undergoing EMT changes, there was chronic fibrosis and tubular atrophy, which was associated with proteinuria and worsening function; however, the relationship between EMT markers and the degree of fibrosis and tubular atrophy, CsA toxicity, and episodes and grade of previous rejections was not clear with the study by Vongwiwatana *et al.*

In contrast, our study used protocol biopsies, not indication-driven biopsies, and primarily focused on early cellular events that lead to graft fibrosis. Previously in other studies, we showed that tubulointerstitial fibrosis at 3 mo is a strong prognostic entity for later graft dysfunction and TID, with acute and subclinical rejection being a strong predictor of graft fibrosis[1,2]; however, in this study, the acute and subclinical rejection rates were relatively low as is often seen with modern immunosuppression. If EMT were driven primarily by rejection,[24,25] as suggested by some and observed in studies of clinically indicated biopsies, then this may explain our modest level of EMT by α-SMA or S100A4 dual staining in protocol biopsies. Another consideration is whether our biopsy time points of 1, 3, and 12 mo were too early, with ischemia-reperfusion injury possibly the cause of the early interstitial fibrosis and missed EMT-induced interstitial fibrosis at later time points. We addressed this concern with a separate substudy from our longitudinal database of 1345 biopsies, in which 20 additional protocol biopsies at 3 mo and 1, 3, 5, and 10 yr were evaluated for EMT by α-SMA, and again observed low-level dual staining similar to the prospective cohort, which remained largely constant over 10 yr despite substantial and progressive increase in cumulative interstitial fibrosis (data not shown). In contrast, when a less specific but more sensitive EMT marker such as S100A4 was used, dual staining was seen much more commonly but was still not followed by subsequent interstitial fibrosis on sequential histology.

This protocol biopsy study using diverse technologies has shown that EMT, although present in varying degrees, was not a major cause of the progressive allograft fibrosis during the first 12 mo after transplantation. Evidence of EMT-associated gene expression was lacking despite use of microarray expression profiles and QRT-PCR. Furthermore, there was no evidence of a causal relationship of EMT with subsequent fibrosis using sequential protocol histology during this early posttransplantation period. Although immune-mediated events remain an important cause of early allograft fibrosis, our observation is that EMT occurs as an isolated event in individual tubular cells, with little evidence of migration into the interstitial space to form a population of myofibroblasts capable of producing interstitial fibrosis. Allograft fibrosis occurred independent of EMT, which does not seem to contribute greatly to early TID.

CONCISE METHODS

Study Population and Protocol Biopsies

The study group consisted of 101 kidney transplants that were performed from June 2003 to July 2005 and for which the recipient was available for at least three sequential protocol kidney biopsies; 55 individuals consented for research. Exclusions from these were absent 3-mo biopsy ($n = 4$), regraft ($n = 2$), protocol biopsy not taken for research ($n = 6$), diabetic donor disease ($n = 1$), RNA unavailable complete protocol series ($n = 1$), recurrence of primary renal disease ($n = 2$), and BK nephropathy on biopsy ($n = 1$), resulting in 36 available patients, 24 of whom were randomly chosen for study. All patients were treated with triple immunosuppression of calcineurin inhibitor, mycophenolate mofetil, and prednisolone. The study was approved by the ethics committee of Western Sydney Area Health Service. This study was in full adherence to the Declaration of Helsinki.

Kidney biopsies were undertaken at implantation and 1, 3, and 12 mo after transplantation. Needle-core protocol biopsies were obtained using an automated biopsy gun with an 18-G needle, under ultrasound guidance. Routine diagnostic tissue samples were taken along with a separate core of renal cortex, immediately snap-frozen, and stored in liquid nitrogen for later microarray and QRT-PCR analysis. One-year protocol renal biopsies were assessed for Banff scores, histology, and dual staining only. Histologic assessment was by a single experienced blinded observer (C.L-S.F.) using the Banff schema[30,31] to determine the extent of interstitial fibrosis and tubular atrophy,[10] referred to here as transplant TID (TID was defined by an individual Banff score of ≥ 1 for both tubular atrophy and interstitial fibrosis).

Study recipients ($n = 24$) were 48.5 $\pm$ 11.9 yr of age with 58% male. The donor age was 47.0 $\pm$ 12.3, and 62.5% were male. The average HLA mismatch score was 3.2 $\pm$ 1.6, cold ischemic time was 331 $\pm$ 288 min, and anastomosis time was 26 $\pm$ 5 min. Delayed fall in serum creatinine (to 150 μmol/L by 10 d) occurred in five (21%) patients, with posttransplantation dialysis required for two (8.3%) of these. Immunosuppression consisted of mycophenolate mofetil and prednisolone in combination with either tacrolimus ($n = 8$ patients/29 biopsies) or CsA ($n = 16/56$). The averaged prevalence rates of subclinical rejection was 16.7% (Banff "borderline" $n = 2$, IA $n = 1$, IB $n = 1$) for both 1 and 3 mo after transplantation. Acute cellular rejection was also seen in 16.7% (Banff IA $n = 2$, IB $n = 2$) for the same time points. The 1-yr serum creatinine was 115 $\pm$ 40 μmol/L and correlated with 3-mo percentage interstitial fibrosis fraction ($r = 0.58$, $P < 0.05$).

Histologic Assessment of EMT and Interstitial Fibrosis

EMT was assessed by dual staining of ECAD and both α-SMA using immunohistochemistry and S100A4 by immunofluorescence on protocol biopsy tissue. Antigen retrieval from paraffin-embedded sections, by automated immunostaining (Discovery XT Immunostainer; Ventana, Tucson, AZ) was followed by blocking of endogenous peroxidases, biotin, and avidin before staining with the primary antibodies, including mouse anti-human α-SMA (clone 1A4; Ventana), visualized with 3,3′diaminobenzidine substrate (as brown), and mouse anti-human ECAD (clone ECH-6; Ventana), visualized with NitroBlue tetrazolium/bromo-chloro-indolylphosphate substrate (as blue). Dual immunofluorescence for ECAD and rabbit anti-human S100A4 (DakoCytomation, Ely, UK) was performed using the rabbit anti-mouse secondary antibodies (DakoCytomation) conjugated to FITC for ECAD visualized as green and swine anti-rabbit conjugated to TRITC (DakoCytomation) for S100A4 visualized as red using confocal microscopy.[11] Control slides were derived from the normal portions of a nephrectomized kidney for renal cell carcinoma. Dual staining for ECAD and α-SMA or S100A4 was assessed by a blinded observer by counting 10 tubules within five high-power (×600) random sampled fields for each biopsy. Samples were classified as EMT positive by the presence of any dual staining for ECAD and α-SMA immunohistochemistry. Because of the greater number of dual staining using immunofluorescence for ECAD and S100A4, an arbitrary cutoff of 15 (median) dual-stained cells per HPF was used to group into severe *versus* minor/absent EMT. Interstitial fibrosis was quantified by morphometric image analysis of multiple Gomori trichrome-stained sections, subject to thresholding of a blue image based on a fixed color combination to standardized estimates, and calculated from area fraction of fibrosis relative to total tubulointerstitial area (Optimas 6a; MedicCybernetics, Sliver Spring, MD).

Gene Expression by cDNA Microarray Analysis

The total RNA was extracted from kidney tissue biopsies using a non-organic column (Micro-to-Midi Total RNA Purification System; Invitrogen, Carlsbad, CA). The mRNA was reverse-transcribed into cDNA using oligo$(dT)_{20}$ primers and reverse transcriptase (SuperScript RNA Amplification System; Invitrogen), followed by linear amplification into complementary-antisense RNA, then assessed for integrity. The cDNA was synthesized using both random hexamers and oligo(dT) in the initial priming step (SuperScript Indirect cDNA Labeling System; Invitrogen). The cDNA hybridization *pairs* (implantation *versus* 1- or 3-mo biopsies) were randomly associated with a *N*-hydroxysuccinimide reactive fluorophore (Cy5 [red] or Cy3

Table 5. QRT-PCR primer sequences for EMT gene expression investigation and cDNA microarray validation[a]

Gene	Primer sequence (5′-3′)	Size (bp)	Function	Accession No.
GAPDH	F-TGCACCACCAACTGCTTAGC R-GGCATGGACTGTGGTCATGAG	87	Housekeeper	[33]
SDHA	F-TGGGAACAAGAGGGCATCTG R-CCACCACTGCATCAAATTCATG	86	Housekeeper	[33]
TGFBR2	F-GCAGGTGGGAACTGCAAGAT R-GAAGGACTCAACATTCTCCAAATTC	76	EMT	[34]
S100A4	F-AACTAAAGGAGCTGCTGACCC R-AAGTCCACCTCGTTGTCCC	118	EMT	BX470102, NM_002961.2
SMAD2	F-CCATCGAAAAGGATTGCC R-ATTCGCAGTTTTCAATTGCC	98	EMT	AF027964, NM_005901.3
BMPR2	F-ACTGGAAATAGACTGGTGCG R-CTTCTAGCACTTCTGGTGCC	94	MET	AC009960, NM_001204.5
TGFB1	F-GCCGCTGCCCATCGTGTACTA R-GGCTTGGGCACGGGTGTCC	193	EMT	BC001180, NM_000660.3
BMP7	F-GATGCAGCGCGAGATCCTC R-CGGCCTTGTAGGGGTAGGAG	170	MET	AF210054, NM_001719.1
MMP2	F-CCCCCAAAACGGACAAAG R-CCGCATGGTCTCGATGGTAT	170	EMT	AY738117, NM_004530.2
BCAT	F-CGGAGACGGAGGAAGGTCTGA R-CACGCTGGATTTTCAAAACAGTTG	149	MET	AY463360, NM_002961.2
RGPS3	F-TACCCTCGCTTTCTCCGTTCT R-CCTCGCTTCCGTATGTCTATCC	216	Array validate	AL359455, NM_144488.4
IGF2	F-GGCCCTCCTGGAGACGTACTGT R-CGGGGTATCTGGGGAAGTTGTC	98	Validation and EMT	AF517226, NM_001042377.1
COL1A2	F-ACAGGGTGCTCGTGGTTTC R-GGCTGTCCCTTCAATCCATC	93	Validation and EMT	M21671, NM_000089.3
SNAIL2 /SLUG	F-ATTCGGACCCACACATTACC R-GAGCCCTCAGATTTGACCT	160	EMT	AF084243, NM_003068.3

[a]BMP7, bone morphogenic protein 7; BMPR2, bone morphogenic protein receptor 2; COL1A2, collagen 1, α 2; GAPDH, glyceraldehyde-3-phosphate dehydrogenase; RGPS3, regulator of G-protein signaling 3; SDHA, succinate dehydrogenase complex, subunit A; SNAIL2/SLUG, snail homolog 2 (*Drosophila*); TGFB1, transforming growth factor-β1; TGFBR2, transforming growth factor-β receptor 2.

[green]; GE Biosciences, Buckinghamshire, UK), followed by cDNA microarray hybridization.

The cDNA microarray slides consisted of 8200 human genes, expression sequence tags, and control spots, all spotted in duplicate (Human 8k cDNA microarrays; AGRF, Melbourne, Australia; using a clone set from ResGen, Invitrogen). The microarray slides were hybridized with labeled cDNA mixed paired samples overnight at 65°C. The cDNA microarrays were scanned by two color GenePix 4000B Microarray Scanner using GenePix6 imaging and analysis program (Agilent Technologies, Santa Clara, CA). Data acquisition was performed using GenePix6. Spots were quantified and quality weighted, and morphologic opening was used for background estimation.

Quantitative Reverse Transcriptase PCR

Reverse transcription and cDNA synthesis were performed using up to 1 μg of total RNA as the initial template for cDNA synthesis (SuperScript III RT; Invitrogen). The primers for the EMT- and MET-associated genes (Table 5) were designed using Oligo6 (Molecular Biology Insights, Cascade, CO) or PRIMER3[32] or obtained from peer-reviewed articles.[33,34] For primer design, the mRNA gene sequences were obtained from GenBank,[35,36] and exact full-sequence alignment was validated by BLASTN.[37]

QRT-PCR was performed on all samples used on the arrays, including those that were inadequate for the arrays ($n = 55$), using SYBR Green I detection system with heat-activated Taq DNA polymerase and uracil DNA glycosylase (Platinum SYBR Green qPCR SuperMix-UDG; Invitrogen). All genes had a unique dissociation curve profile. Absolute quantification with standard curve was used, normalizing against two housekeeping genes (glyceraldehyde-3-phosphate dehydrogenase and succinate dehydrogenase complex, subunit A) and internal control (implantation sample) for all genes tested. Standard curves for both housekeeper and test samples were $\log_{10}$ dilutions of PCR product plotting cycle threshold (Ct) *versus* $\log_{10}$ (copy-number) producing tight correlations ($R^2 = 0.98$ to 0.99) for all curves. The lower detection limit of the QRT-PCR was 10^{-8} for both glyceraldehyde-3-phosphate dehydrogenase and succinate dehydrogenase complex, subunit A based on pooled test cDNA.

Statistical Analysis

For cDNA microarray analysis, differential gene expression was analyzed (Bioconductor 1.8[38] incorporating LIMMA[39] on the R2.2.1 statistical computing environment[40]), where genes were ranked by B value and adjusted *P* value. The LIMMA analysis was performed on samples according to transplant TID status (both TID and normal [no TID] were investigated). Differentially expressed gene lists were interrogated using DAVID,[41] SOURCE,[42] GeneCards,[43] Entrez PubMed (http://www.ncbi.nlm.nih.gov) and Significance Analysis of Microarrays,[44] specifically focusing on EMT genes, and data were subgrouped according to TID and EMT status and compared with normal in each case. The gene expression output from differentially expressed genes with a $B > 1$ or isolated EMT-associated genes was subject to hierarchical clustering (Cluster 3.0[45]), and results were visualized (TreeView 1.60[46]).

Raw QRT-PCR results were $\log_e$ converted and analyzed using a paired two-tailed *t* test or single-tailed Mann-Whitney *U*/Wilcoxon test. Data stratified by TID status on biopsy were analyzed using linear-by-linear association with a one-sided Monte Carlo test for significance. Data were expressed as means ± SD unless otherwise stated. $P < 0.05$ was considered significant for general statistical analyses. *Post hoc* probabilities are presented for microarray analyses.

ACKNOWLEDGMENTS

Department of Renal Medicine and Centre for Transplant and Renal Research is a member of the Clinical Centre for Research Excellence in Renal Medicine, which is funded by the National Health and Medical Research Council of Australia and the National Institutes of Health (grant no. UO1-AI070107-01).

We thank Helen Robertson and John Kirby for providing the immunofluorescence protocol and advice. We gratefully acknowledge Dr. Gopi Rangan for use of the image analysis software and equipment. M.V. specifically thanks his family, wife Laurice Gamit, and God for their continued love, support, and understanding.

DISCLOSURES

P.J.O. received consulting fees from Wyeth, lecture fees from Janssen-Cilag, and a grant from Roche. J.R.C. has received consulting and lecture fees from Novartis, Roche, Fujisawa, and Wyeth; lecture fees from Janssen-Cilag; and a grant from Novartis.

REFERENCES

1. Nankivell BJ, Borrows RJ, Fung CL, O'Connell PJ, Allen RD, Chapman JR: The natural history of chronic allograft nephropathy. *N Engl J Med* 349: 2326–2333, 2003
2. Nankivell BJ, Fenton-Lee CA, Kuypers DR, Cheung E, Allen RD, O'Connell PJ, Chapman JR: Effect of histological damage on long-term kidney transplant outcome. *Transplantation* 71: 515–523, 2001
3. Neilson EG: Setting a trap for tissue fibrosis. *Nat Med* 11: 373–374, 2005
4. Liu Y: Epithelial to mesenchymal transition in renal fibrogenesis: Pathologic significance, molecular mechanism, and therapeutic intervention. *J Am Soc Nephrol* 15: 1–12, 2004
5. Yang J, Liu Y: Dissection of key events in tubular epithelial to myofibroblast transition and its implications in renal interstitial fibrosis. *Am J Pathol* 159: 1465–1475, 2001
6. El-Nahas AM: Plasticity of kidney cells: Role in kidney remodeling and scarring. *Kidney Int* 64: 1553–1563, 2003
7. Iwano M, Plieth D, Danoff TM, Xue C, Okada H, Neilson EG: Evidence that fibroblasts derive from epithelium during tissue fibrosis. *J Clin Invest* 110: 341–350, 2002
8. Vongwiwatana A, Tasanarong A, Rayner DC, Melk A, Halloran PF: Epithelial to mesenchymal transition during late deterioration of human kidney transplants: The role of tubular cells in fibrogenesis. *Am J Transplant* 5: 1367–1374, 2005
9. Djamali A, Reese S, Yracheta J, Oberley T, Hullett D, Becker B: Epithelial-to-mesenchymal transition and oxidative stress in chronic allograft nephropathy. *Am J Transplant* 5: 500–509, 2005
10. Solez K, Colvin RB, Racusen LC, Sis B, Halloran PF, Birk PE, Campbell PM, Cascalho M, Collins AB, Demetris AJ, Drachenberg CB, Gibson

IW, Grimm PC, Haas M, Lerut E, Liapis H, Mannon RB, Marcus PB, Mengel M, Mihatsch MJ, Nankivell BJ, Nickeleit V, Papadimitriou JC, Platt JL, Randhawa P, Roberts I, Salinas-Madriga L, Salomon DR, Seron D, Sheaff M, Weening JJ: Banff '05 Meeting Report: Differential diagnosis of chronic allograft injury and elimination of chronic allograft nephropathy ('CAN'). *Am J Transplant* 7: 518–526, 2007
11. Tyler JR, Robertson H, Booth TA, Burt AD, Kirby JA: Chronic allograft nephropathy: Intraepithelial signals generated by transforming growth factor-beta and bone morphogenetic protein-7. *Am J Transplant* 6: 1367–1376, 2006
12. Liu Y: Renal fibrosis: New insights into the pathogenesis and therapeutics. *Kidney Int* 69: 213–217, 2006
13. Medici D, Hay ED, Goodenough DA: Cooperation between snail and LEF-1 transcription factors is essential for TGF-beta1-induced epithelial-mesenchymal transition. *Mol Biol Cell* 17: 1871–1879, 2006
14. Eger A, Stockinger A, Schaffhauser B, Beug H, Foisner R: Epithelial mesenchymal transition by c-Fos estrogen receptor activation involves nuclear translocation of beta-catenin and upregulation of beta-catenin/lymphoid enhancer binding factor-1 transcriptional activity. *J Cell Biol* 148: 173–188, 2000
15. Valcourt U, Kowanetz M, Niimi H, Heldin CH, Moustakas A: TGF-beta and the Smad signaling pathway support transcriptomic reprogramming during epithelial-mesenchymal cell transition. *Mol Biol Cell* 16: 1987–2002, 2005
16. Rhyu DY, Yang Y, Ha H, Lee GT, Song JS, Uh ST, Lee HB: Role of reactive oxygen species in TGF-beta1-induced mitogen-activated protein kinase activation and epithelial-mesenchymal transition in renal tubular epithelial cells. *J Am Soc Nephrol* 16: 667–675, 2005
17. Legrand O, Simonin G, Zittoun R, Marie JP: Lung resistance protein (LRP) gene expression in adult acute myeloid leukemia: A critical evaluation by three techniques. *Leukemia* 12: 1367–1374, 1998
18. Novotny GW, Sonne SB, Nielsen JE, Jonstrup SP, Hansen MA, Skakkebaek NE, Rajpert-De Meyts E, Kjems J, Leffers H: Translational repression of E2F1 mRNA in carcinoma in situ and normal testis correlates with expression of the miR-17–92 cluster. *Cell Death Differ* 14: 879–882, 2007
19. Bhattacharyya SN, Habermacher R, Martine U, Closs EI, Filipowicz W: Relief of microRNA-mediated translational repression in human cells subjected to stress. *Cell* 125: 1111–1124, 2006
20. Novotny GW, Nielsen JE, Sonne SB, Skakkebaek NE, Rajpert-De Meyts E, Leffers H: Analysis of gene expression in normal and neoplastic human testis: New roles of RNA. *Int J Androl* 30: 316–326, discussion 326–327, 2007
21. Bartel DP: MicroRNAs: Genomics, biogenesis, mechanism, and function. *Cell* 116: 281–297, 2004
22. Draghici S, Khatri P, Eklund AC, Szallasi Z: Reliability and reproducibility issues in DNA microarray measurements. *Trends Genet* 22: 101–109, 2006
23. van Bakel H, Holstege FC: In control: Systematic assessment of microarray performance. *EMBO Rep* 5: 964–969, 2004
24. Robertson H, Ali S, McDonnell BJ, Burt AD, Kirby JA: Chronic renal allograft dysfunction: The role of T cell-mediated tubular epithelial to mesenchymal cell transition. *J Am Soc Nephrol* 15: 390–397, 2004
25. Hertig A, Verine J, Mougenot B, Jouanneau C, Ouali N, Sebe P, Glotz D, Ancel PY, Rondeau E, Xu-Dubois YC: Risk factors for early epithelial to mesenchymal transition in renal grafts. *Am J Transplant* 6: 2937–2946, 2006
26. Grimm PC, Nickerson P, Jeffery J, Savani RC, Gough J, McKenna RM, Stern E, Rush DN: Neointimal and tubulointerstitial infiltration by recipient mesenchymal cells in chronic renal-allograft rejection. *N Engl J Med* 345: 93–97, 2001
27. McMorrow T, Gaffney MM, Slattery C, Campbell E, Ryan MP: Cyclosporine A induced epithelial-mesenchymal transition in human renal proximal tubular epithelial cells. *Nephrol Dial Transplant* 20: 2215–2225, 2005
28. Slattery C, Campbell E, McMorrow T, Ryan MP: Cyclosporine A-induced renal fibrosis: a role for epithelial-mesenchymal transition. *Am J Pathol* 167: 395–407, 2005
29. Muramatsu M, Miyagi M, Ishikawa Y, Aikawa A, Mizuiri S, Ohara T, Ishii T, Hasegawa A: Estimation of damaged tubular epithelium in renal allografts by determination of vimentin expression. *Int J Urol* 11: 954–962, 2004
30. Racusen LC, Colvin RB, Solez K, Mihatsch MJ, Halloran PF, Campbell PM, Cecka MJ, Cosyns JP, Demetris AJ, Fishbein MC, Fogo A, Furness P, Gibson IW, Glotz D, Hayry P, Hunsickern L, Kashgarian M, Kerman R, Magil AJ, Montgomery R, Morozumi K, Nickeleit V, Randhawa P, Regele H, Seron D, Seshan S, Sund S, Trpkov K: Antibody-mediated rejection criteria: An addition to the Banff 97 classification of renal allograft rejection. *Am J Transplant* 3: 708–714, 2003
31. Racusen LC, Solez K, Colvin RB, Bonsib SM, Castro MC, Cavallo T, Croker BP, Demetris AJ, Drachenberg CB, Fogo AB, Furness P, Gaber LW, Gibson IW, Glotz D, Goldberg JC, Grande J, Halloran PF, Hansen HE, Hartley B, Hayry PJ, Hill CM, Hoffman EO, Hunsicker LG, Lindblad AS, Yamaguchi Y, *et al.*: The Banff 97 working classification of renal allograft pathology. *Kidney Int* 55: 713–723, 1999
32. Australian National Genome Information Service (ANGIS). Sydney Bioinformatics, University of Sydney, 2006. Available at: http://www.angis.org.au. Accessed April 25, 2006
33. Vandesompele J, De Preter K, Pattyn F, Poppe B, Van Roy N, De Paepe A, Speleman F: Accurate normalization of real-time quantitative RT-PCR data by geometric averaging of multiple internal control genes. *Genome Biol* 3: RESEARCH0034, 2002
34. Huang C, Kim Y, Caramori ML, Fish AJ, Rich SS, Miller ME, Russell GB, Mauer M: Cellular basis of diabetic nephropathy: II. The transforming growth factor-beta system and diabetic nephropathy lesions in type 1 diabetes. *Diabetes* 51: 3577–3581, 2002
35. Wheeler DL, Barrett T, Benson DA, Bryant SH, Canese K, Chetvernin V, Church DM, DiCuccio M, Edgar R, Federhen S, Geer LY, Helmberg W, Kapustin Y, Kenton DL, Khovayko O, Lipman DJ, Madden TL, Maglott DR, Ostell J, Pruitt KD, Schuler GD, Schriml LM, Sequeira E, Sherry ST, Sirotkin K, Souvorov A, Starchenko G, Suzek TO, Tatusov R, Tatusova TA, Wagner L, Yaschenko E: Database resources of the National Center for Biotechnology Information. *Nucleic Acids Res* 34: D173–D180, 2006
36. Benson DA, Karsch-Mizrachi I, Lipman DJ, Ostell J, Wheeler DL: GenBank. *Nucleic Acids Res* 34: D16–D20, 2006
37. Altschul SF, Gish W, Miller W, Myers EW, Lipman DJ: Basic local alignment search tool. *J Mol Biol* 215: 403–410, 1990
38. The BioConductor core team: BioConductor. Available at: http://www.bioconductor.org
39. Smyth GK, Michaud J, Scott, HS: Use of within-array replicate spots for assessing differential expression in microarray experiments. *Bioinformatics* 21: 2067–2075, 2005
40. R Development Core Team: The R Project for Statistical Computing. Available at: http://www.r-project.org
41. Dennis G Jr, Sherman BT, Hosack DA, Yang J, Gao W, Lane HC, Lempicki RA: DAVID: Database for Annotation, Visualization, and Integrated Discovery. *Genome Biol* 4: P3, 2003
42. Diehn M, Sherlock G, Binkley G, Jin H, Matese JC, Hernandez-Boussard T, Rees CA, Cherry JM, Botstein D, Brown PO, Alizadeh AA: SOURCE: A unified genomic resource of functional annotations, ontologies, and gene expression data. *Nucleic Acids Res* 31: 219–223, 2003
43. Rebhan M, Chalifa-Caspi V, Prilusky J, Lancet D: *GeneCards: Encyclopedia for Genes, Proteins and Diseases*, Rehovot, Israel, Weizmann Institute of Science, Bioinformatics Unit and Genome Centre, 1997
44. Tusher VG, Tibshirani R, Chu G: Significance analysis of microarrays applied to the ionizing radiation response. *Proc Natl Acad Sci U S A* 98: 5116–5121, 2001
45. Eisen M, Imoto S, Miyano S: *Cluster 3.0*, Stanford, Stanford University, 1998–1999, 2002
46. Eisen M: *TreeView 1.60*, Stanford, Stanford University, 2002